Mathematical Medicine and Biology (2018) **35**, 203–224
doi:10.1093/imammb/dqw025
Advance Access publication on 18 February 2017

Early treatment gains for antibiotic administration and within human host time series data

TODD R. YOUNG* AND ERIK M. BOCZKO
Mathematics, Ohio University, 321 Morton, Athens, Ohio 45701, USA
*Corresponding author. Email: youngt@ohio.edu

[Received on 4 March 2016; revised on 21 October 2016; accepted on 30 December 2016]

As technological improvements continue to infiltrate and impact medical practice, it has become possible to non-invasively collect dense physiological time series data from individual patients in real time. These advances continue to improve physicians' ability to detect and to treat infections early. One important benefit of early detection and treatment of nascent infections is that it leads to earlier resolution. In response to current and anticipated advances in data capture, we introduce the Early Treatment Gain (ETG) as a measure to quantify this benefit. Roughly, we define the gain to be the limiting ratio:

$$\text{ETG} = \frac{\text{differential change in time of resolution}}{\text{differential change in treatment time}}.$$

We study the gain using standard dynamical models and demonstrate its use with time series data from Surgical Intensive Care Unit (SICU) patients facing ventilator associated pneumonia. The main conclusion from the mathematical modelling is that the ETG is always greater than one unless there is an effective immune response, in which case the ETG can be less than one. Using real patient time series data, we observe that the formula derived for a linear model can be applied and that this produces a ETG greater than one.

Keywords: pulmonary infection; dynamical systems; differential equations; ventilator associated pneumonia.

1. Introduction

1.1 *Background*

It is often the case in medical practice that early detection and treatment of a disease results in a favourable outcome. In some cases, most notably cancer, early diagnosis is highly corollated with survival and it is thus clear that "earlier is better". As another example, it is known that starting antiretroviral therapy early in response to HIV infection not only prevents serious AIDS-related diseases, but also prevents the onset of several non-AIDS-related diseases such as cancer and cardiovascular disease (INSIGHT START Study Group, 2015)

In recent years, a few tools have been developed that quantify benefits of treatment to patients, such as the quality-adjusted life-year (QALY) and the EuroQol five dimensions questionnaire (EQ-5D) a standardized instrument for measuring generic health status in the face of chronic conditions. QALYs gained is used as an outcome in cost-utility analysis (Whynes, 2008) Analogous measures have been employed for many years in the treatment of psychological disorders such as schizophrenia (Heinrichs *et al.*, 1984)

© The authors 2017. Published by Oxford University Press on behalf of the Institute of Mathematics and its Applications. All rights reserved.

Many infectious diseases, e.g. syphilis, are reliably curable with antimicrobial therapy and many others are resolved by the patient's immune system alone, without the need for antibiotics. Even in such cases it is still perhaps the case that earlier treatment is beneficial to the patient. One might wish to quantify the benefits of early treatment for the patient so that physicians might balance the benefits with the possibility of side-effects and the imperative to limit antibiotic exposure (Leekha *et al.*, 2011) It seems that quantitative measures for benefits of treatment have focused entirely on reliability of elimination of the infection (Khan *et al.*, 2002) In this manuscript, we propose a new measure (the ETG, see below) of the benefit of early treatment that seeks to quantify the effects of early treatment in terms of the time to resolution.

We illustrate the new measure by applying it to newly available real time-series data from ventilated SICU patients. These data sets predict that earlier treatment would have been highly beneficial to these ventilated patients in terms of time to resolution of the infections and overall exposure to the infecting pathogens.

1.2 *Mathematical definitions and notation*

Suppose that an infected patient is administered an effective treatment beginning at time t and that as a result the infection is resolved at time T. Assuming further that T is a differentiable function of t, i.e. $T(t)$, we define the 'Early Treatment Gain', $\mathrm{ETG}(t)$, by:

$$\mathrm{ETG}(t) = T'(t).$$

The reason for this name can be seen by considering the following. Suppose the patient had been treated at a slightly earlier time $t - \delta$. Then, still assuming smoothness of $T(t)$, we have that

$$\frac{T(t) - T(t-\delta)}{\delta} \approx \mathrm{ETG}(t) \qquad \text{or} \qquad T(t) - T(t-\delta) \approx \mathrm{ETG}(t)\delta.$$

The ETG approximates the ratio of the time to resolution to the treatment time differential. (It also estimates the ratio of increase of time to resolution if the treatment is delayed.) For example, ETG = 1.5 would mean that if effective treatment is administered 1 day earlier, the infection would be resolved approximately 1.5 days earlier. On the other hand, it also means, e.g. that a 6 h delay in treatment would result in approximately additional 9 h of infection.

Note that ETG is a non-dimensional number used as a multiplier.

The differential quantity $\mathrm{ETG}(t)$ is related to a more global notion of early treatment gain on some time interval $[t_1, t_2]$ by:

$$\frac{T(t_2) - T(t_1)}{t_2 - t_1} = \frac{1}{t_2 - t_1} \int_{t_1}^{t_2} \mathrm{ETG}(t)\, dt = \overline{\mathrm{ETG}},$$

where $\overline{\mathrm{ETG}}$ denotes the mean value of $\mathrm{ETG}(t)$ on the interval $[t_1, t_2]$.

Our definition does not specify the term 'resolved.' The formulation of the ETG is consistent with any measurable criteria of the patient's state that depends smoothly on time, in the context of bacterial infections by 'resolved' we mean that the bacterial load reaches some fixed small value, denoted by χ.

TABLE 1 *List of main notations used*

$t_0 \equiv 0$	time of beginning of infection
$t_1 > 0$	time of initiation of antibiotic treatment
$x(t_1)$	pathogen load at the start of antibiotic treatment
χ	bacterial load below which the infection is resolved
$T(t_1)$	time of resolution, depends on t_1 and χ
ETG $\equiv T'(t_1)$	the early treatment gain
α	(linear) growth rate of bacteria (Section 2)
a	(linear) effectiveness of treatment (Section 2)
$y(t)$	immune response (Section 3 and Section 4)

2. Gains in the absence of an immune response

2.1 *Basic models*

Assume that the patient's bacterial load follows a trajectory defined by one autonomous differential equation up until the time of treatment, after which it follows a trajectory defined by a second autonomous equation after the treatment. In other words:

$$\begin{aligned} x' &= f(x), \quad 0 \le t < t_1 \\ x' &= f_a(x), \quad t_1 < t \le T. \end{aligned} \tag{2.1}$$

Presumably, $f(x) > 0$ and $f_a(x) < 0$ for all $x > 0$.

Proposition 2.1 For the system (2.1) and the assumptions $f(x) > 0$ and $f_a(x) < 0$ for $x > 0$, then early treatment gain is given explicitly by:

$$\mathrm{ETG}(t_1) = 1 + \frac{x'(t_1^-)}{|x'(t_1^+)|}. \tag{2.2}$$

In this equation, $x'(t_1^-) = \lim_{t \to t_1^-} x'(t)$, i.e. the limiting slope before treatment and $x'(t_1^+) = \lim_{t \to t_1^+} x'(t)$, the limiting slope after treatment.

Proof. Let $\delta \neq 0$ and consider the system where we begin treatment at $t_1 + \delta$. Then,

$$\mathrm{ETG}(t_1) = \lim_{\delta \to 0} \frac{T(t_1 + \delta) - T(t_1)}{\delta}.$$

Let $x_1 = x(t_1)$ and $x_2 = x(t_1 + \delta)$. Note that $x(t)$ will decrease for $t > t_1 + \delta$ and must equal x_1 for exactly one $t = t_1 + \delta + \delta'$. Now note that the initial value problems

$$x' = f_a(x), \quad x(t_1) = x_1$$

and

$$x' = f_a(x), \quad x(t_1 + \delta + \delta') = x_1$$

will have exactly the same solution except shifted in time by $\delta + \delta'$. Thus, we have that

$$T(t_1 + \delta) - T(t_1) = \delta + \delta',$$

and so,

$$\frac{T(t_1 + \delta) - T(t_1)}{\delta} = 1 + \frac{\delta'}{\delta}.$$

Next, consider that (see for instance (Perko, 2000, Section 2.1)):

$$x_2 = x_1 + \int_{t_1}^{t_1+\delta} f(x(s))\, ds \quad \text{and} \quad x_1 = x_2 + \int_{t_1+\delta}^{t_1+\delta+\delta'} f_a(x(s))\, ds,$$

and therefore,

$$\int_{t_1}^{t_1+\delta} f(x(s))\, ds = \int_{t_1+\delta}^{t_1+\delta+\delta'} -f_a(x(s))\, ds.$$

By the mean value theorem for integrals, there exist τ_1 and τ_2 such that $t_1 < \tau_1 < t_1 + \delta$, $t_1 + \delta < \tau_2 < t_1 + \delta + \delta'$, and

$$f(x(\tau_1))\delta = -f_a(x(\tau_2))\delta'.$$

Therefore, it follows that:

$$\frac{\delta'}{\delta} = \frac{x'(\tau_1)}{-x'(\tau_2)},$$

and so, by smoothness,

$$\lim_{\delta \to 0} \frac{\delta'}{\delta} = \frac{x'(t_1^-)}{|x'(t_1^+)|},$$

where $x(t)$ is the solution with treatment at t_1. ■

Of particular note from the patient's perspective is that the gain, in this case is always greater than one. The decrease/increase in time to resolution is greater than the differential of time in beginning treatment.

For simplistic, but useful, bacterial growth models such as linear or logistic it is straightforward to compute the treatment time explicitly from the solutions. In spite of their simplicity, the results offer insights into the nature of early treatment gains.

2.2 *Linear model*

Consider a *linear model system*, where the pathogen grows at a constant rate of $\alpha > 0$ in the absence of treatment. We will consider that α may include the constant inhibitory effects from the innate immune system. We may interpret α as the natural growth rate of the pathogen in the host, with no adaptive response.

Suppose that after treatment the bacteria decay with rate $\alpha - a < 0$, with the assumptions that $a > \alpha > 0$. Here a can be thought of as the effectiveness of the treatment.

$$\begin{aligned} x' &= \alpha x, & x(0) &= x_0, & 0 \le t \le t_1, \\ x' &= (\alpha - a)x, & x(t_1) &= x(t_1), & t_1 \le t. \end{aligned} \tag{2.3}$$

The well known solutions are

$$\begin{aligned} x(t) &= x_0 e^{\alpha t}, \quad 0 \le t \le t_1 \\ x(t) &= x_0 e^{\alpha t_1}) e^{(\alpha - a)(t - t_1)} \\ &= x_0 e^{a t_1} e^{(\alpha - a)t}, \quad t_1 \le t. \end{aligned}$$

Setting $x(T) = \chi$ ($\chi < x(t_1)$) and solving for T explicitly we obtain:

$$T = \frac{a}{a - \alpha} t_1 + \frac{1}{a - \alpha} \ln \frac{x_0}{\chi}.$$

In this case, we see that T is linear in the treatment time t_1 and while T depends on both t_1 and χ, the gain depends on neither, nor does it depend on the amount of pathogen at the time of treatment. It depends only on the ratio of the growth rates before and after treatment.

$$\mathrm{ETG}_{linear} \equiv \frac{dT}{dt_1} = \frac{a}{a - \alpha} = 1 + \frac{\alpha}{a - \alpha}. \tag{2.4}$$

It is straightforward to show that this result agrees with Equation (2.2).

Figure 1 illustrates the gain in the linear case and a simple geometric argument using similar triangles can be used to derive the gain. It suggests how the ETG might be inferred from patient data by simple linear fitting of the rise and fall of the bacterial load. In particular, if the bacterial load rises and falls exponentially, the rate of growth $\alpha > 0$ and rate of decrease $\alpha - a < 0$ are easily interpreted as slopes in the plot of $\ln x$ vs. t.

2.3 *Area under the curve of the bacterial load*

In addition to the ETG, one might consider other measures of the benefits of earlier treatment, such as the overall length and severity of the infection. A natural measure corresponding to this would be the area under the curve (AUC) of the bacterial load $x(t)$. AUC is a commonly used measure in various contexts of medical practice and research such as the interpretation of statistical ROC curves (Cali & Longobardi, 2015), pharmacokinetics (Swan, 1988; Lappin *et al.*, 2006) and many others (Nani & Oğuztöreli, 1999; Bungay *et al.*, 2003; Oleinick *et al.*, 2006; Maki *et al.*, 2008; Eleanor *et al.*, 2011; Kuznetsov, 2013). We have not found the AUC of infectious load in the medical literature, but the 'area under the disease progression curve' is used in accessing the severity of blight and parasite attacks on crops (Meenaa *et al.*, 2011).

In the linear model, the AUC of $\ln x(t)$ in Fig. 1 is easily interpreted and calculated as the area of triangles. Using the level $\ln \chi$ as the base, the triangle corresponding to treatment beginning at t_1 has area

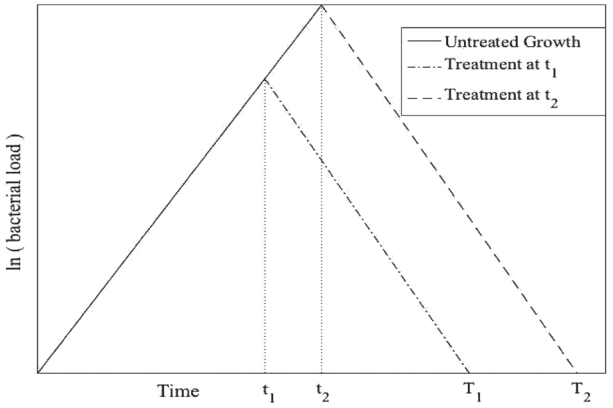

FIG. 1. Sketch of a log-linear plot of the exponential growth model as described in System (2.3). Growth (solid) and decay curves become linear with slopes corresponding to the growth and decay rates, $\alpha > 0$ and $\alpha - a < 0$, respectively. Pictured are two curves corresponding to two different treatment times t_1 (dashed-dotted) and t_2 (dashed). The hypothetical infections are resolved when the curves reach χ (small baseline value) at $T_1 = T(t_1)$ and $T_2 = T(t_2)$. The gain can be computed as $\text{ETG} = \frac{T_2 - T_1}{t_2 - t_1} = 1 + \frac{\alpha}{a - \alpha}$. We show in Section 2.3 that the difference in the areas under the curves in these two graphs, i.e. the area of the quadrilateral with bottom corners at T_1 and T_2 is proportional to the ETG.

$AUC = \frac{1}{2} h_1 T_1$, where h_1 is the height of the triangle and T_1 is the length of its base. Considering that $h_1 = \alpha t_1$ and $T_1 = \text{ETG}\, t_1$ we obtain:

$$AUC = \frac{\alpha}{2} t_1^2 \,\text{ETG}.$$

As a consequence,

$$\frac{dAUC}{dt_1} = \alpha t_1 \,\text{ETG}.$$

If we consider the area $\mathcal{AUC}$ under the curve $x(t)$ rather than $\ln x(t)$, then a direct calculation shows that

$$\mathcal{AUC} = \chi\,(e^{\alpha t_1} - 1)\,\text{ETG} \quad \text{and} \quad \frac{d}{dt_1}\mathcal{AUC} = \alpha\,\chi\, e^{\alpha t_1}\,\text{ETG}$$

Note that $\chi \exp \alpha t_1$ is precisely the peak bacterial load in this model.

Thus, we conclude that the AUC of the bacterial load varies directly with the ETG in the linear case.

2.3.1 *Higher dimensional linear models* The result above generalizes to higher dimensional linear systems, and we describe the solution here for completeness. Consider a system of linear systems in two or more dimensions. Without loss of generality, we consider each dimension to describe a different species of pathogen.

$$\begin{aligned} x' &= Ax, & x(0) &= x_0, & 0 \le t \le t_1 \\ x' &= A_a x, & x(t_1) &= x(t_1), & t_1 \le t \end{aligned} \tag{2.5}$$

Using the properties of matrix exponentials the solution is conveniently described as $x(t) = \exp(t - t_1)A_a \exp t_1 A x_0$ for $t > t_1$.

If, e.g. we wish to consider the resolution of the first pathogen, then projecting onto the first dimension we obtain: $\chi = \langle x(T), e_1 \rangle$, and differentiating with respect to t_1 to obtain:

$$0 = \langle (A + (\mathrm{ETG} - 1)A_a)x(T), e_1 \rangle$$

and

$$\mathrm{ETG} = 1 - \frac{\langle Ax(T), e_1 \rangle}{\langle A_a x(T), e_1 \rangle} \tag{2.6}$$

Under the natural assumptions that $\langle Ax, e_1 \rangle > 0$ and $\langle A_a x, e_1 \rangle < 0$, the gain is greater than one. This formula collapses to $\mathrm{ETG} = 1 + \frac{\alpha}{a-\alpha}$ if (2.5) is reduced to a scalar system.

2.4 *Logistic model*

Next, we study a logistic system that incorporates a carrying capacity K that models growth restriction based on host environment conditions. We note that some conditions can be manipulated by the host, e.g. by iron sequestration (Skaar, 2010). Consider the system:

$$\begin{aligned} x' &= \alpha x \left(1 - \frac{x}{K}\right), & x(0) &= x_0, & 0 \le t \le t_1 \\ x' &= \alpha x \left(1 - \frac{x}{K}\right) - ax, & x(t_1) &= x(t_1), & t_1 \le t. \end{aligned} \tag{2.7}$$

This system might be an appropriate model in case of infections that are persistent but not fatal.

Setting $x(T) = \chi$, using $r = a - \alpha$, $C = Kr/\alpha$, and continuing to assume that $a > \alpha > 0$ and $\chi < x(t_1)$ leads to the relation:

$$-r(T - t_1) = \ln \frac{C + x(t_1)}{x(t_1)} + \ln \frac{\chi}{C + \chi}.$$

Differentiating, we find:

$$\begin{aligned} \mathrm{ETG} = \frac{dT}{dt_1} &= 1 - \frac{1}{a-\alpha}\left(\frac{x'(t_1)}{C + x(t_1)} - \frac{x'(t_1)}{x(t_1)}\right) \\ &= 1 + \frac{1}{a-\alpha}\left(\frac{1}{x(t_1)} - \frac{1}{C + x(t_1)}\right)x'(t_1) \\ &= 1 + \frac{1}{a-\alpha}\left(\frac{1}{x(t_1)} - \frac{1}{C + x(t_1)}\right)\alpha x(t_1)\left(1 - \frac{x(t_1)}{K}\right) \\ &= 1 + \left(\frac{\alpha}{a-\alpha}\right)\left(1 - \frac{x(t_1)}{K}\right)\left(1 - \frac{x(t_1)}{C + x(t_1)}\right). \end{aligned}$$

Here too the early treatment gain is always greater than 1, given the assumptions. If $x(t_1)$ is small then the value of the ETG is close to that derived for the linear model. However, as $x(t_1)$ approaches the

carrying capacity K, the ETG approaches 1 from above. Thus, the benefits of early treatment diminish if the infection remains untreated. Regardless of how one chooses to model the antibiotic induced decay, the same conclusion remains. For example, using $f_a(x) = (\alpha - a)x$ the resulting gain is ETG $= 1 + (\frac{\alpha}{a-\alpha})(1 - \frac{x(t_1)}{K})$. The phenomena can be understood by considering again the geometry in Fig. 1. If the bacterial growth reaches a plateau then two parallel lines of decay reach resolution in virtually the same amount of time.

3. Infection with a programmed immune response

Assume that the initial bacterial growth within the host, prior to treatment and prior to immune surveillance is exponential with constant growth rate α. Further, make the modelling assumption that an adaptive immune response is triggered when the pathogenic load reaches a threshold level and that once this response is triggered it follows a predetermined response i.e. thereafter insensitive to the bacterial density (Boldrick *et al.*, 2002; Nau *et al.*, 2002).

Without loss of generality, we may call the threshold level x_0 and assume that the response is triggered at time $t = 0$. If we let y denote the effectiveness of the immune response in inhibiting growth of the pathogen, then given the assumptions, y is a fixed function of time $y(t)$. For the adaptive response, we would generally expect $y(0) = 0$ and for $y(t)$ to remain zero for some amount of time on the order of a few days. Once the adaptive response begins to ramp up, we expect it to increase monotonically and then to level off at a maximum level $y(\infty)$. In essence, we expect that y can be approximated by a sigmoidal (S-shaped) function (also called 'Hill-type function') of t.

Given this setting, it is natural to consider the distinct cases in which $y(\infty)$ is either greater than or less than α, i.e. the adaptive response is sufficient or insufficient to eliminate the pathogen. In either case, we examine the model :

$$\begin{aligned} x' &= (\alpha - y(t))x, & x(0) &= x_0, & 0 \le t \le t_1 \\ x' &= (\alpha - y(t) - a)x, & x(t_1) &= x(t_1), & t_1 \le t. \end{aligned} \tag{3.1}$$

Solving for $x(T)$, and setting $x(T) = \chi$ we arrive at the relation

$$\ln(\frac{\chi}{x_0}) = \alpha t_1 + (\alpha - a)(T - t_1) - \int_0^T y(s)ds.$$

Differentiating with respect to t_1, we arrive at

$$\text{ETG} = 1 + \frac{\alpha - y(T)}{a - (\alpha - y(T))}. \tag{3.2}$$

The magnitude of the early treatment gain is greatly influenced by whether or not the immune response by itself is sufficient to clear the pathogen. If $y(t) > \alpha$ for t reasonably small (on the order of a few days), then the ETG will be less than one. On the other hand, if $y(t) < \alpha$ for all t then the ETG will greater than one. Also note if $y(t)$ is indeed increasing, then the earlier the treatment, the larger the ETG. If the infection could be resolved solely by the patient's immune system, then the differential benefits of antibiotic therapy smaller than for cases where the treatment is necessary for resolution.

4. Models with predator-prey type immune response

Pugliese & Gandolfi (2008) introduced the following equations to model the interaction between a pathogen and the host's immune response:

$$\begin{aligned} x' &= \alpha x - \frac{mx}{1+\beta_u x} - \frac{x}{1+\beta_s x} y \\ y' &= -y + \frac{x}{1+\gamma x} y + \eta. \end{aligned} \tag{4.1}$$

Here, $x(t)$ is the density of the pathogen load, and $y(t)$ is the density of cells of the adaptive system. The pathogen is exponentially replicating with rate α. Elimination of the pathogen due to the adaptive system is captured by the term $-xy/(1+\beta_s x)$. Production of y is stimulated by presence of the pathogen as represented by the term $xy/(1+\gamma x)$. The small term η represents the adaptive system's base level production of cells (needed to keep y from going to zero). These parts of the equations represent a standard type of predator-prey modelling. Inclusion of the term $mx/(1+\beta_u x)$ models the elimination of the pathogen by the innate immune response, which occurs immediately upon pathogen detection. This term is immediate in its effect. Even with the inclusion of this term, the equations are still only two dimensional and qualitative (phase-diagram) analysis of the equations (Pugliese & Gandolfi, 2008) can be completed. One property is that if $\alpha < m$, then the equilibrium with $x = 0$ is locally stable. Thus, the model correctly reproduces the phenomenon that the innate system can eliminate small pathogen loads. The model also captures the diminishing effectiveness of the innate system on larger pathogen loads (since $mx/((1+\beta_u x) \to 1$ as x becomes large). A shortcoming of the model (4.1) is that the interaction terms are specific. D'onofrio (2010) generalized the model (4.1) to allow for more flexible functions representing the interactions. In Appendix A we investigate models with a more general immune response.

Next, assume that after the treatment begins, the growth rate α in (4.1) is replaced by a negative term $\alpha - a$. Thus, the post treatment dynamics are governed by:

$$\begin{aligned} x' &= (\alpha - a)x - \frac{mx}{1+\beta_u x} - \frac{x}{1+\beta_s x} y \\ y' &= -y + \frac{x}{1+\gamma x} y + \eta. \end{aligned} \tag{4.2}$$

We note that it is impossible to obtain an explicit solution for such equations and in Fig. 2, we illustrate numerical solutions. In the first panel the parameters are such that the infection will grow indefinitely. In the second panel, the infection is eventually resolved by the immune system response. In each of these panels, solution curves are shown with treatment beginning at times $t = 1, 2, \ldots, 8$ (days) and never.

We observe in Fig. 2(a) and (b) that some of the solutions may cross in the t,x-plane. This indicates that early treatment could lead to a prolonged resolution (in this model). This happens because of differing levels of immune responses; in this model earlier treatment lowers the overall immune response. In Fig. 2(c), we plot the level of immune response over time from the same simulations as in Fig. 2(a). In Fig. 2(d), we show estimates of the ETG from simulations of the model formulated in (4.1) and (4.2). Here, the parameters are set as in (a), a case where the infection would not be controlled. Most notable in this plot is that the ETG is lower than one for the treatment times in an intermediate range. We provide programs for these simulations in Appendix B.

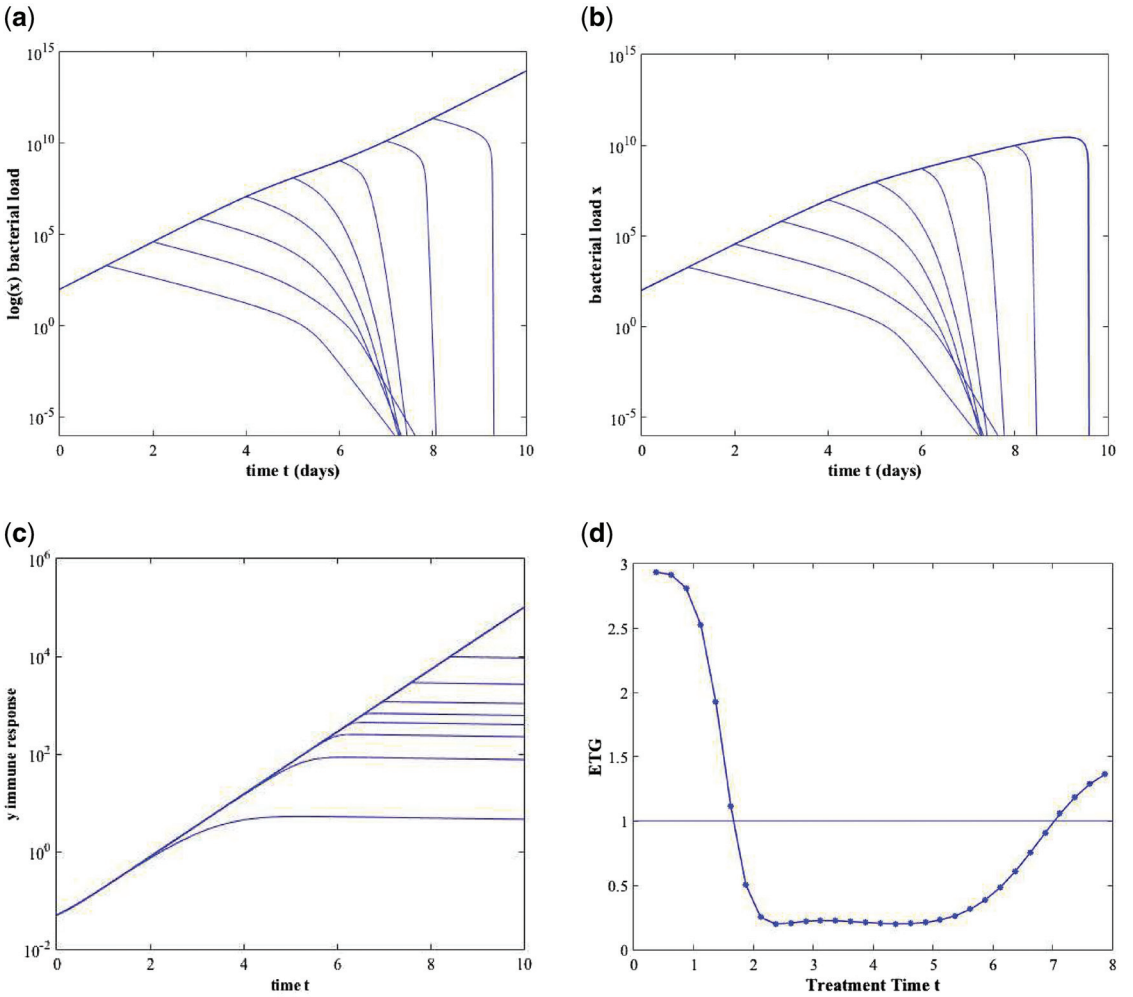

FIG. 2. Examples of bacterial load of solutions of the systems (4.1) and (4.2) with antibiotic treatment starting at times $t = 1, 2, \ldots, 8$. In (a) and (b), the top curve is $x(t)$ without treatment. In both panels, the initial conditions are $(100, \eta)$ and the parameters are $\eta = 0.05$, $\gamma = 0.02$, $\beta_s = 10^{-8}$, $\beta_u = 2$, $m = 200$ and $a = -150$. In (a) $\alpha = 100$ and the infection is not controlled by the immune system. In panel (b) $\alpha = 98.273$ and the infection is eventually controlled by the immune system alone. In panels (a) and (b), the departure from the untreated curve is due to the administration of the antibiotic. The subsequent change in slope is due to the immune response. (c) The level of immune response $\log(y)$ over time under in the simulation for subfigure (a) with treatment initiated at $t = 1, 2, \ldots, 8$. In this model earlier treatment attenuates the immune response. (d) Early Treatment Gains $\mathrm{ETG}(t_1)$ for subfigure (a) estimated from the numerical solutions. In the presence of an immune response the ETG may be subject to surprising non-linear effects.

We observe from these simulations that an adaptive immune response may have an unexpected nonlinear effect on the ETG. For many treatment times the ETG that we estimate from this model are significantly greater than one. But for some treatment times the differential quantity ETG is compressed by the ramp-up of the immune response. Comparing Fig. 2(c) with Fig. 2(a), we see that for treatment beginning in the range 2–6 days solutions display a 'focusing' effect that results in the dip in $\mathrm{ETG}(t_1)$. This

happens even though the immune response is not strong enough to eliminate the infection. Figure 2(c) shows that this model predicts that the immune system stops ramping up soon after effective antibiotic treatment is begun.

5. Estimating ETG from patient time series

5.1 *Ventilator associated pneumonia and ventilator filters*

Having investigated the early treatment gain in several mathematical models, we demonstrate the utility of the ETG in the context of actual patient time series.

Critically ill patients requiring mechanical ventilation are at significant risk for developing ventilator associated pneumonia (VAP). Only a few years ago, VAP was the second most common hospital acquired infection of critically ill patients (Koenig & Truwit, 2006) and affected 27% of all critically ill patients (Richards *et al.*, 1999). VAP markedly increases ventilator, Intensive Care Unit, and hospital days, as well as mortality. The excess health care costs of VAP and other nosocomial infections are large and well documented (Stone, 2009).

Improvements in intensive care practice have greatly decreased the incidence of VAP, but serious obstacles remain, including the fact that there does not exist an accessible biomarker that correlates well with initial infections. Part of the difficulty in identifying such biomarkers has been that the lungs strongly compartmentalize the innate and early adaptive immune response (Zhang *et al.*, 2000). Recently, however, it has been observed that pathogens and biomarkers are constantly shed in aerosolized droplets that are rich in alveolar lining fluid. In ventilated patients, these droplets accumulate in the ventilator circuit, and can be collected and assayed (Isaacs *et al.*, 2012; Young *et al.*, 2012).

Time series derived from the aerosolized alveolar lining fluid (AALF) droplets display the rise and fall of the bacterial load, along with the predator-prey type dynamics that characterizes the conflict between the bacteria and the immune system. As a result of the availability of this type of physiological data that captures, at least in part, the process of bacterial growth and its response to antibiotic therapy, we can use the methods formulated here to predict how the bacterial load would respond to an antibiotic challenge presented at an earlier or later time point.

5.2 *Time series from SICU patients*

Time series data were collected from patients in the SICU at Vanderbilt University Medical Center, as convenience samples within a larger comparative study designed to test the efficacy of estimating pathogenic load from AALF. Details of the data collection can be found in Isaacs *et al.* (2012); May *et al.* (2015). Briefly, self-contained sterile filters placed in the ventilator circuit accumulate aerosolized droplets of alveolar lining fluid shed from the lungs during respiration. Filters were collected from patients by the study team at different time points during their hospital stay. The fluid contents of the filters were analysed for bacterial load and composition using quantitative Polymerase chain reaction (PCR). Aerosolized alveolar lining fluid contains many host biomarkers in addition to the bacterial load. In this article, we present data that allows us to begin to understand how the host immune system interacts with the bacterial load in real time.

In all of the patient trajectories, a large dot indicates the results of a bronchial alveolar lavage (BAL). The standard VAP protocol calls for a BAL to be performed in response to elevated temperature and white cell count, plus at least one of the several other physiological indicators known to correlate with VAP. The performance of a BAL, as opposed to AALF collection, is an invasive procedure that requires intubation and is not suitable for serial sampling. Our previous work has validated that the non-invasive

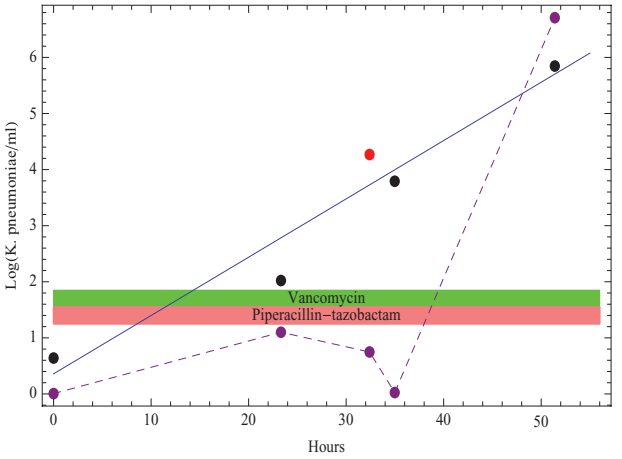

FIG. 3. An AALF derived time series collected from patient A reveals the growth of *K. pneumoniae*. Black dots represent the bacterial load ($\log_{10}$ CFU/ml) detected from AALF samples. The grey dot indicates the load from a BAL sample. The dashed line shows the quantity of bacterial endotoxin from AALF samples. Antibiotic type and duration is depicted by bars. Apparently the antibiotic treatment given during this time span was not effective since the bacteria load persistently increased. The load is well-approximated by exponential growth.

AALF samples agree with results obtained from time-matched BAL samples (Isaacs *et al.*, 2012; May *et al.*, 2015). That agreement can also be seen in these time series data.

Patient A

Patient A was infected with *Klebsiella pneumoniae* as evidenced by the rising bacterial load in Fig. 3. The serial AALF samples were also assayed for the presence of bacterial endotoxin. The endotoxin signal plateaus prior to the BAL and is seen to be in decline just prior to spiking after the BAL. The solid black line is a linear regression of bacterial load.

The data indicate that the bacterial load is rising despite antibiotic treatment. The patient A data illustrate two important points: (1) time-series of the bacterial load within a human host can be collected accurately and non-invasively (2) bacterial growth, in this patient, during this time period, is roughly exponential. An approximation of the bacterial growth rate was easily extracted from the slope of the regression line. The *K. pneumoniae* are seen to grow at a rate of $\alpha \approx 0.1/\text{hr}$.

Patient B

The data from patient B, Fig. 4 are far more detailed. Roughly 6 days after the bacterial load began to increase, near the height of the infection, patient B passed a spontaneous breathing trial and met the extubation criteria and was subsequently extubated at the time point indicated by the grey dot at 6 days. Following extubation, the patient's pulmonary function rapidly declined and the patient was subsequently re-intubated, a BAL was performed and empiric antibiotic therapy was initiated as displayed in the figure. Both the BAL and the AALF serial samples confirmed that the patient was infected with both *Enterobacter cloacae* and *Staphylococcus aureus*. The AALF time series data shown could have been of utility to the physicians managing this patient.

From patient B's time course, Fig. 4, the rate of bacterial growth, $\alpha \approx 0.03/\text{hr}$, and the rate of bacterial decline, $\alpha - a \approx -0.022/\text{hr}$, were regressed. Using these values, we calculate an early treatment gain of $\text{ETG} = 1 + \alpha/|\alpha - a| \approx 2.3$ for this patient. This value suggests that had the patient been given this

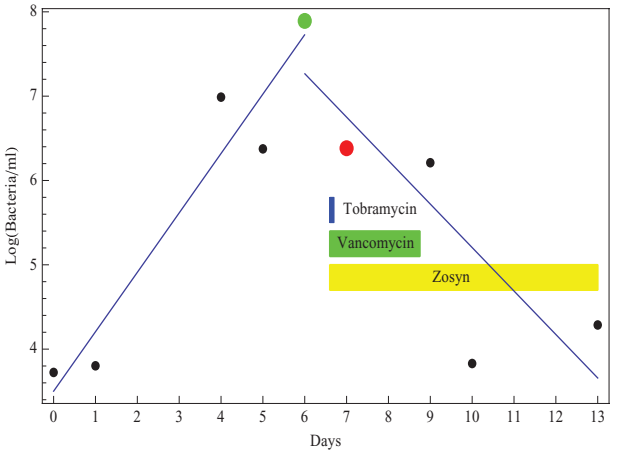

FIG. 4. Patient B. The black dots indicate the combined bacterial load (log_{10} CFU/ml) of *E. cloacae* and *S. aureus*) from AALF. The second large dot indicates a BAL. The patient was extubated at the first large dot. The solid regression lines predicts an ETG of 2.3 using Equation 2.4. Antibiotic administration is indicated by bars.

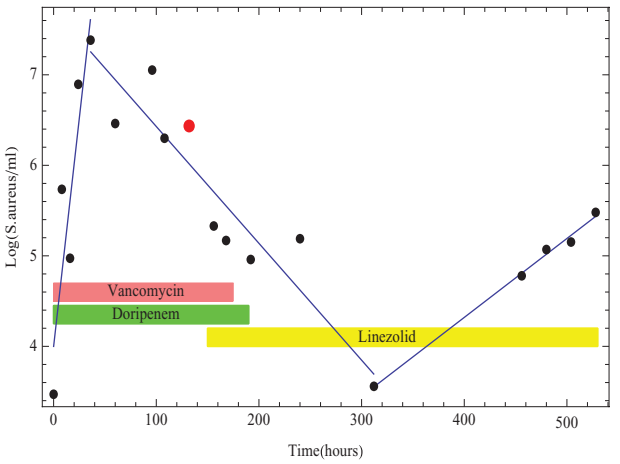

FIG. 5. Patient C. Black dots indicate the *S. aureus* load ($\log_{10}$ CFU/ml) from AALF samples. The large dot differentiates the matching BAL. The solid regression lines were used to estimate growth rate. Antibiotics administration is indicated by bars. For this patient that improvement and decline do not coincide precisely with beginning and end of antibiotic treatments.

course of antibiotics a day earlier, the patients bacterial load would have resolved 2.3 days earlier. Had the therapy begun 2 days earlier the infection might have resolved 4.6 days earlier.

Patient C

The data from patient C, Fig. 5 illustrates that the AALF time series has the potential to detect the onset of infection AND the effectiveness of its treatment. The *S. aureus* infection in patient C was determined to be HAII-MRSA by MLST analysis. The MRSA display a rapid initial growth rate with

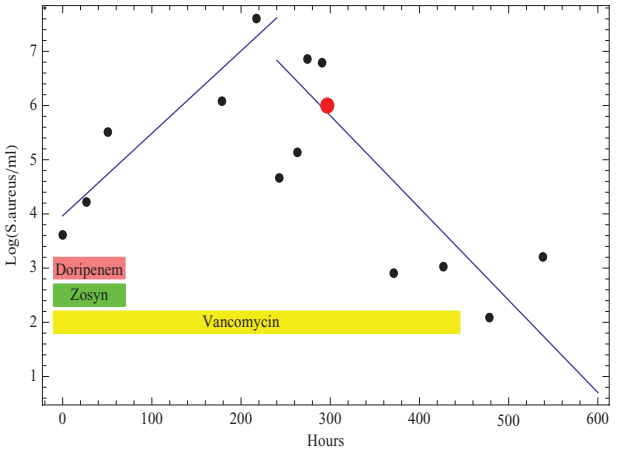

FIG. 6. Patient D. The black dots are *S. aureus* (log 10 CFU/ml) from AALF samples. The large dot indicates a BAL. Again the improvement and decline of the patient does not precisely track the antibiotic treatment. The data in this case also seem to be fairly noisy.

a doubling time of 3 h in the face of vancomycin therapy for a remote infection. Clinical deterioration of the patient's pulmonary status, near 125 h, triggered the performance of a BAL that revealed greater than 10^6 CFU/ml of MRSA (CFU = Colony Forming Units) and prompted a conversion of the empiric therapy to Linezolid. Despite the Linezolid treatment the MRSA rebounded near 300 h, albeit at a slower rate. A genetic analysis of the AALF samples from these time points revealed the presence of a Linezolid resistant strain of MRSA.

From the linear regression shown in Fig. 5, we obtain the rate of bacterial growth, $\alpha \approx 0.098/\text{h}$, and the rate of bacterial decline, $\alpha - a \approx -0.013/\text{h}$, to calculate an early treatment gain of $\text{ETG} = 1 + \alpha/|\alpha - a| \approx 8.5$ for this patient.

There are several additional observations of note in the patient C data. First, the initial turning point of the infection, i.e. near 40 h, does not coincide with the initiation or change in antibiotic therapy. A cause and effect understanding of this phenomenon requires more data. Second, after the rebound the bacterial growth is exponential with an estimated growth rate of $\alpha \approx .0086/\text{hr}$. The variance of the data about the regression line is completely different than that seen in the other patient data, and in patient C at the earlier time points.

Patient D

Patient D provides another more detailed example of a co-infection, consisting of a combination of *S. aureus* and *P. aeruginosa*. The data from this patient are presented in Figs 6 and 7. These figures combine to illustrate the correlated dynamics of the bacterial growth and the host immune system.

The regression estimate of the *S. aureus* growth rate is, $\alpha \approx 0.015/\text{hr}$, and the estimate of its rate of decline is, $\alpha - a \approx 0.017/\text{hr}$. These estimates produce an early treatment gain of $\text{ETG} = 1 + \alpha/|\alpha - a| \approx 1.9$ for patient D.

In all of the patient data, A–D presented in this article, we measured and observed cytokine spikes that are temporally correlated with changes in the bacterial growth rate, as shown for patient D in Fig. 7.

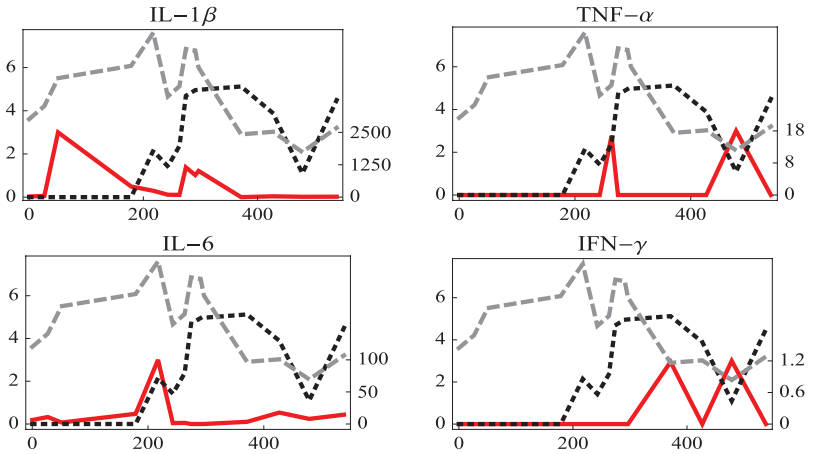

FIG. 7. An AALF time series from Patient D. In each panel the dashed gray line indicates the growth of *S. aureus* as shown in Fig. 6. The dashed black line indicates the growth of *P. aeruginosa*. The amount of bacteria per ml of AALF fluid are represented on a log scale (base 10) on the left axis. The solid line in each panel represents the level of a specific cytokine in pg/ml, with the scale on the right. The plots reveal the interplay between the infection and immune response.

6. Conclusions and discussion

The main conclusion from the mathematical modelling and analysis is that the Early Treatment Gain is greater than one unless there is an effective immune response, in which case the ETG can be less than one. The results point to the importance of the immune system—an effective immune response seems to dominate effective treatment in the ETG analysis. This was seen in two different mathematical models of the immune system; programmed immune response and predator-prey type infection/immune dynamics. But, in cases where an effective immune response is not forthcoming or is much delayed, the early treatment is predicted to produce clear benefits in terms of time to resolution.

In Section 2.3, we demonstrated that an AUC measurement of bacterial load in the infection is directly proportional to the ETG in situations where the growth and decay curves of the infection are exponential.

The predator-prey model of the infection-immune response process, predicts that it is possible for antibiotic treatment to delay the resolution of an infection. In the mathematical model, this is due to the attenuation of the immune response if the treatment is given just as the immune response is ramping up. It is clearly of interest, beyond validating the mathematical model, to understand whether or not this counter-intuitive effect occurs in actual infections.

The lungs are normally a nearly sterile environment and individual microorganisms are cleared by the components of the innate immune system, particularly by neutrophils and alveolar macrophages (Craig *et al.*, 2009). Pulmonary infections begin when this process fails and pathogens succeed in establishing a foothold within one or more alveolar sacs. Because the innate immune response takes place at the level of individual interactions between extremely small numbers of cells, stochastic modelling is probably more relevant (see Wood *et al.* 2014). An Ordinary Differential Equation (ODE) model, as we have used throughout this manuscript, might only become appropriate after an infection has begun. At the point where detection is possible from clinical capture of aerosolized samples of alveolar fluid or from any other method, the number of bacteria in the lungs is no longer small, as can be seen in the patient data presented, and thus our ODE modelling is reasonable in the context under investigation.

Estimates of the ETG are readily calculated for most patient time series from the simple formula derived for a linear model. In the cases, we examined the estimates produce an ETG of greater than one. The implication for ventilated SICU patients is that early treatment results in resolution i.e. earlier than that expected from a simple shift backward in time, e.g. if we had started the same therapy one day earlier, the infection would have resolved one day earlier. Since the onset of a pulmonary infection in ventilated patients can eventually result in ventilator associated pneumonia, a condition with serious consequences, the benefits of earlier detection may also have an additional advantage in terms of the morbidity and mortality of the patient Stone (2009). In patients B–D, we calculated ETG values ranging between 2–8. These values are large and offer the possibility to significantly shorten SICU days. The benefits of the ETG are not simply limited to significantly shortening the length of hospital stays. It is also likely that early treatment will allow infections to be handled with 'less' antibiotic exposure, because an order of magnitude in exponential growth is meaningful. These potential benefits demonstrates the true promise of non-invasive serial sampling.

Analysis of the time series data has revealed some very interesting phenomena that offer opportunities for future research. As an example, we return to the observation made in patient C, regarding the nature of the bacterial growth after the rebound. The growth in this phase of the infection is markedly and significantly statistically different. The low variance in the growth rate closely resembles that seen in growth curves measured for single strains of bacteria growing unimpeded in a flask with ample nutrients. This suggests two, not mutually exclusive, possibilities. One possibility is that the prolonged and varied antibiotic exposure has homogenized the bacterial population thus reducing strain induced variations in growth rate. Another possibility is that host immune system has collapsed, allowing the strain to grow unimpeded as it would in a flask in the lab. To imagine this latter possibility compare driving with one foot versus two. One foot gives a smoother ride. Further investigation is clearly required, and warranted, to determine the true nature of this observation.

The AALF time series offer the opportunity to quantitatively study the nature of bacterial infections in a human host. Surprisingly, there are very few articles in the literature describing the process with the level of quantitative detail as we have presented for patients A–D. For example, estimates from poultry (Lindqvist, 2006), indicate that the growth rates of *S. aureus* vary greatly by strain, and may have doubling times as fast as 2.6 h. There are similar data for rabbits and mice, but most of the studies contain 3–5 data points in time, and very few replicates. We have not been able to find similar data for bacterial growth rates within human hosts in the current literature.

Acknowledgements

We thank the anonymous referees for their careful consideration of an earlier draft and numerous helpful suggestions that led to the substantial improvement of this manuscript.

Funding

E.B. was funded by the Vanderbilt Institute for Clinical and Translational Research (VICTR), (CTSA 1 UL1 RR024975). E.B. and T.Y. received support from an NIH-NIGMS grant R01 GM090207.

References

Boldrick, J. C., Alizadeh, A., Diehn, M. & et al. (2002). Stereotyped and specific gene expression programs in human innate immune responses to bacteria. *Proc. Natl. Acad. Sci. USA.,* **99**, 972–977.

BUNGAY, S. D., GENTRY, P. A. & GENTRY, R. D. (2003). A mathematical model of lipid-mediated thrombin generation. *Math. Med. Biol.,* **20**, 105–129.

CALI, C. & LONGOBARDI, M. (2015) Some mathematical properties of the ROC curve and their applications. *Ricerche Mat.* **64**, 391–402.

CRAIG, A., MAI, J., CAI, S. S. & JEYASEELAN, S. (2009). Neutrophil recruitment to the lungs during bacterial pneumonia. *Infect. Immun.*, **77**, 568–575.

D'ONOFRIO, A. (2010). On the interaction between the immune system and an exponentially replicating pathogen. *Math. Biosci. Bioeng.,* **7** 579–602.

ELEANOR A. J., BOSTON, E. A. J. & GAFFNEY, E. A. (2011). The influence of toxicity constraints in models of chemotherapeutic protocol escalation. *Math. Med. Biol.,* **28**, 357–384.

HEINRICHS, D. W., HANLON, T. E. & CARPENTER, B. N. (1984). The Quality of Life Scale: an instrument for rating the schizophrenic deficit syndrome. *Schizophr Bull.,* **10**, 388–398.

The INSIGHT START Study Group (2015). Initiation of Antiretroviral Therapy in Early Asymptomatic HIV Infection. *N. Engl. J. Med.,* **373**, 795–807.

ISAACS, R. J., DEBELAK, K., NORRIS, P. R., JENKINS, J. M., ROOKS, J. C., YOUNG, T. R., MAY, A. K. & BOCZKO, E. M. (2012). Non-Invasive detection of pulmonary pathogens in ventilator-circuit filters by PCR. *Am. J. Translat. Res.,* **4**, 72–82.

KHAN, W. A., SAHA, D., RAHMAN, A., SALAM, M. A., BOGAERTS, J. & BENNISH, M. L. (2002). Comparison of single-dose azithromycin for childhood cholera: a randomized, double-blind trial. *Lancet*, **360**, 1722–1727.

KOENIG, S. & TRUWIT, J. (2006). Ventilator-associated pneumonia: diagnosis, treatment, and prevention. *Clin. Microbiol. Rev.,* **19**, 637–657.

KUZNETSOV, A. V. (2013). Modelling of axonal cargo rerouting in a dendrite. *Math. Med. Biol.,* **30**, 273–285.

LAPPIN, G., ROWLAND, M. & GARNER, R. C. (2006). The use of isotopes in the determination of absolute bioavailability of drugs in humans. *Expert Opin. Drug Metab. Toxicol.,* **2**, 419–427.

LEEKHA, S., TERRELL, C. L. & EDSON, R. S. (2011). General principles of antimicrobial therapy. *Mayo Clin. Proc.,* **86**, 156–167.

LINDQVIST, R. (2006). Estimation of *Staphylococcus aureus* growth parameters from turbidity data: characterization of strain variation and comparison of methods. *Appl. Environ. Microbiol.,* **72**, 4862–4870.

MAKI, K. L., BRAUN, R. J., DRISCOLL, T. A. & KING-SMITH, P. E. (2008). An overset grid method for the study of reflex tearing. *Math. Med. Biol.,* **25**, 187–214.

MAY, A. K., BRADY, J. S., ROMANO-KEELER, J., DRAKE, W. P., NORRIS, P. R., JENKINS, J. M., ISAACS, R. J. & BOCZKO, E. M. (2015). A pilot study of the non-invasive assessment of the lung microbiota as a potential tool for the early diagnosis of ventilator associated pneumonia. *Chest*, **147**, 1494–1502.

MEENAA, P. D., CHATTOPADHYAYA, C., MEENAA, S. S. & KUMARA, A. (2011). Area under disease progress curve and apparent infection rate of Alternaria blight disease of Indian mustard (Brassica juncea) at different plant age. *Arch. Phytopathol. Plant Protect.,* **44**, 684–693.

NANI, F. K. & OĞUZTÖRELI, M. N. (1999). Modelling and simulation of chemotherapy of haematological and gynaecological cancers. *Math. Med. Biol.*, **16** 39–91.

NAU, G. J., RICHMOND, J. F. L., SCHLESINGER, A. & ET AL. (2002). Human macrophage activation programs induced by bacterial pathogens. *Proc. Natl. Acad. Sci. USA.,* **99**, 1503–1508.

OLEINICK, A. I., AMATORE, C., GUILLE, M., ARBAULT, S., KLYMENKO, O. V. & SVIR, I. (2006). Modelling release of nitric oxide in a slice of rat's brain: describing stimulated functional hyperemia with diffusion-reaction equations. *Math. Med. Biol.,* **23**, 27–44.

PERKO, L. (2000). *Differential Equations and Dynamical Systems, 3rd edn*. Texts in Applied Mathematics 7. New York: Springer.

PUGLIESE, A. & GANDOLFI, A. (2008). A simple model of pathogen-immune dynamics including specific and non-specific immunity. *Math. Biosci.,* **214**, 73–80.

RICHARDS, M. J., EDWARDS, J. R., CULVER, D. H., GAYNES, R. P. & ET AL. (1999). Nosocomial infections in medical intensive care units in the United States. *Crit. Care Med.,* **27**, 887–892.

SKAAR, E. P. (2010). The battle for iron between bacterial pathogens and their vertebrate hosts. *PLoS Pathog.,* **6**, e1000949.

STONE, P. W. (2009). Economic burden of healthcare-associated infections: an American perspective. *Expert Rev. Pharmacoecon Outcomes Res.,* **9**, 417–422

SWAN, G. W. (1988). General Applications of Optimal Control Theory in Cancer Chemotherapy. *Math. Med. Biol.,* **5**, 303–316.

WHYNES, D. K. (2008). Correspondence between EQ-5D health state classifications and EQ VAS scores. *Health Qual. Life Outcomes,* **6**, 94.

WOOD, R. M., EGAN, J. R. & HALL, I. M. (2014). A dose and time response Markov model for the in-host dynamics of infection with intracellular bacteria following inhalation: with application to Francisella tularensis. *J. R. Soc. Interface,* **11**, 20140119.

YOUNG, T. R., BUCKALEW, R., MAY, A. K. & BOCZKO, E. M. (2012). A low dimensional dynamical model of the pulmonary innate immune response to infection. *Math. Biosci.,* **235**, 189–200.

ZHANG, P., SUMMER, W., BAGBY, G. & NELSON, S. (2000). Innate immunity and pulmonary host defense. *Immun. Rev.*, **173**, 39–51.

Appendix A. General models with immune response

Next we consider

$$\begin{aligned} x' &= f(x,y), \quad y' = g(x,y), \qquad 0 \le t \le t_1 \\ x' &= f_a(x,y), \quad y' = g(x,y), \qquad t_1 \le t. \end{aligned} \tag{A.1}$$

As in Section 2.1, suppose that treatment is begun instead at time $t_1 + \delta$ where $\delta > 0$ is small. Let us adopt the notation $(x_1, y_1) = (x(t_1), y(t_1))$ and make the assumption that $f(x_1, y_1) > 0$ and $f_a(x_1, y_1) < 0$. Let also $(x_2, y_2) = (x(t_1+\delta), y(t_1+\delta))$ and note that $x_2 > x_1$. There is then $\delta' > 0$ such that $x(t_1+\delta+\delta') = x_1$. During the same time period $y(t)$ will change. Let $y_3 = y(t_1 + \delta + \delta')$, then it follows that:

$$\begin{aligned} y_3 &= y_1 + (\delta + \delta')g(x_1, y_1) + O(\delta + \delta')^2, \\ &= y_1 + \delta(1 + \frac{\delta'}{\delta})y'(t_1) + O(\delta^2), \\ &= y_1 + \delta\left(1 + \frac{x'(t_1^-)}{|x'(t_1^+)|}\right)y'(t_1) + O(\delta^2). \end{aligned}$$

Now at time $t + \delta + \delta'$ we can treat the problem as an IVP:

$$x' = f_a(x,y), \quad y' = g(x,y), \qquad x(t_1 + \delta + \delta') = x_1, y(t_1 + \delta + \delta') = y_3 \tag{A.2}$$

This initial value problem is equivalent to the same IVP shifted to t_1:

$$x' = f_a(x,y), \quad y' = g(x,y), \qquad x(t_1) = x_1, \quad y(t_1) = y_3 \tag{A.3}$$

The solution of this IVP at time T will satisfy:

$$x(T) = \tilde{x}(T) + \frac{\partial \tilde{x}(T)}{\partial y_1}(y_3 - y_1).$$

Where we let $\tilde{x}$ denote the original solution with $y(t_1) = y_1$. We may obtain that the solution of the IVP (A.2) satisfies:

$$x(T+\delta+\delta') \approx \chi + \frac{\partial \tilde{x}(T)}{\partial y_1}\delta\left(1+\frac{x'(t_1^-)}{|x'(t_1^+)|}\right)y'(t_1).$$

The term $\partial\tilde{x}(T)/\partial y_1$ will be negative since increasing y_1 corresponds to increasing the immune response. So, we have $x(T+\delta+\delta') < \chi$. Let δ'' be the increment of time such that: $x(T+\delta+\delta'-\delta'') = \chi$. We have the δ'' is approximated by:

$$\begin{aligned}\delta'' &= \frac{x(T+\delta+\delta')-\chi}{x'(T)} \\ &= \frac{y'(t_1)}{x'(T)}\delta\left(1+\frac{x'(t_1^-)}{|x'(t_1^+)|}\right)\frac{\partial\tilde{x}(T)}{\partial y_1}.\end{aligned} \tag{A.4}$$

Thus we have that the time at which the solution of (A.2) satisfies $x(t) = \chi$ is

$$T+\delta+\delta'-\delta'' = T+\delta\left(1+\frac{\delta'}{\delta}\right)+\frac{y'(t_1)}{|x'(T)|}\frac{\partial\tilde{x}(T)}{\partial y_1}\delta\left(1+\frac{x'(t_1^-)}{|x'(t_1^+)|}\right)$$

or

$$T+\delta+\delta'-\delta'' = T+\delta\left(1+\frac{x'(t_1^-)}{|x'(t_1^+)|}\right)\left(1+\frac{y'(t_1)}{|x'(T)|}\frac{\partial\tilde{x}(T)}{\partial y_1}\right).$$

The early treatment gain is then:

$$\mathrm{ETG}(t_1) = \left(1+\frac{x'(t_1^-)}{|x'(t_1^+)|}\right)\left(1+\frac{y'(t_1)}{|x'(T)|}\frac{\partial\tilde{x}(T)}{\partial y_1}\right).$$

Unfortunately, the term $\partial\tilde{x}(T)/\partial y_1$ can only be obtained by solving the variational equation:

$$\frac{d}{dt}\Phi = DF(x(t),y(t))\Phi, \qquad \Phi(t_1) = I,$$

where F is the full vector field (f,g). However, we do know that this term should be negative, which again leads to the conclusion that $\mathrm{ETG}(t_1)$ is smaller in the presence of an effective immune response. On the other hand, if $\partial\tilde{x}(T)/\partial y_1$ is small then the ETG reduces to that predicted in equation (2.2) .

Appendix B. Matlab programs

The following code will produce the plots in Fig. 2 with (a) $\alpha = 100$ or (b) $\alpha = 98.273$.

```
% PGsim_plots
% initialize parameters
alpha = 98.273;
```

```
m = 200;
beta_s = 10^(-8);
beta_u= 2;
gam = 0.02;
eta = 0.05;

% set initial condition
Y0 = [100 ; eta]

% f1 and f2 are the diff eqns before and after treatment
options = odeset('RelTol',1e-8,'AbsTol',1e-8)
f1=@(t,y) .03*[alpha*y(1)-((y(1)*y(2))/(1+beta_s*y(1)))
                         -((m*y(1))/(1+beta_u*y(1)));
                           (y(1)*y(2))/(1+gam*y(1))-y(2)+eta]
f2=@(t,y) .03*[-.5*alpha*y(1)-((y(1)*y(2))/(1+beta_s*y(1)))
                             -((m*y(1))/(1+beta_u*y(1)));
                               (y(1)*y(2))/(1+gam*y(1))-y(2)+eta]

for i=1:8

% timespan
tspan1 = [0 i] % before treatment
tspan2 = [i 10] % after treatment

% Integrate system before treatment
[TT,YY] = ode45(f1,tspan1,Y0,options);
X = YY(:,2);

semilogy(TT,X,'LineWidth',1)
pbaspect([1 .85 1])
xlabel('t','fontsize',20,'fontweight','b')
ylabel('log(y)','fontsize',20,'fontweight','b')
hold on

% Integrate after treatment
Y1 = YY(max(size(TT)),:);
[TT,YY] = ode45(f2,tspan2,Y1, options);
YY = max(YY,zeros(size(YY))+.0000001);
X = YY(:,2);
semilogy(TT,X,'LineWidth',1)
end

% Integrate without treatment
tspan = [0 10]
[TT,YY] = ode45(f1,tspan,Y0);
YY = max(YY,zeros(size(YY))+.0000001);
```

```
X = YY(:,2);
semilogy(TT,X,'LineWidth',1.5)
```

The next MATLAB program will produce the plot of the ETG in Fig. 2(d).

```
% PGintegration
% initialize parameters
alpha = 100;
m = 200;
beta_s = 10^(-8);
beta_u= 2;
gam = 0.02;
eta = 0.05;

% set initial condition
Y0 = [100 ; eta]
Tstop = [];

% Set tolerance. f1 and f2 are the diff eqns before and after
treatment. options=odeset('RelTol',1e-8,'AbsTol',1e-8)
f1=@(t,y) .03*[alpha*y(1)-((y(1)*y(2))/(1+beta_s*y(1)))
                         -((m*y(1))/(1+beta_u*y(1)));
                           (y(1)*y(2))/(1+gam*y(1))-y(2)+eta]

f2=@(t,y) .03*[-.5*alpha*y(1)-((y(1)*y(2))/(1+beta_s*y(1)))
                            -((m*y(1))/(1+beta_u*y(1)));
                              (y(1)*y(2))/(1+gam*y(1))-y(2)+eta]

h = .00001;
Y = Y0;
T=0;
y = Y(1,1)

% solution with immediate treatment
while y > 1
   k1 = f2(T,Y);
   k2 = f2(T+h/2,Y+k1*h/2);
   k3 = f2(T+h/2,Y+k2*h/2);
   k4 = f2(T+h,Y+k3*h);
   Y = Y+h*(k1+2*k2+2*k3+k4)/6;
   T = T+h;
   y = Y(1,1);
end
Tstop = [Tstop T]

for i=1:30
```

```
% integrate up to treatment time
tspan1 = [0 .5*i]
[TT,YY] = ode45(f1,tspan1,Y0,options);

% integrate with treatment until resolution
Y = YY(max(size(TT)),:)'
T = TT(max(size(TT)),:)
y = Y(1,1)
while y > 1
   k1 = f2(T,Y);
   k2 = f2(T+h/2,Y+k1*h/2);
   k3 = f2(T+h/2,Y+k2*h/2);
   k4 = f2(T+h,Y+k3*h);
   Y = Y+h*(k1+2*k2+2*k3+k4)/6;
   T = T+h;
   y = Y(1,1);
end
Tstop = [Tstop T]
end

t = [0:.5:15];
tmid = (t(2:31)+t(1:30))/2;
ETG = (Tstop(2:31) - Tstop(1:30))/.5;

plot(tmid,ETG,'*-','LineWidth', 1.5)

hold on
t = 0:1:15;
plot(t,ones(size(t)))

xlabel('Treatment Time','fontsize',20,'fontweight','b')
ylabel('ETG','fontsize',20,'fontweight','b')
pbaspect([1 .8 1])
```